FISEVIER

Contents lists available at ScienceDirect

Optics and Lasers in Engineering

journal homepage: www.elsevier.com/locate/optlaseng



A cylindrical neighborhood for multi-view range images processing



Bao-Quan Shi a,b,*, Jin Liang b

- ^a School of Electro-Mechanical Engineering, Xidian University, Xi'an 710071, Shaanxi, PR China
- ^b State Key Laboratory for Manufacturing Systems Engineering, Xi'an Jiaotong University, Xi'an 710049, Shaanxi, PR China

ARTICLE INFO

Article history:
Received 10 May 2014
Received in revised form
13 August 2014
Accepted 24 September 2014
Available online 17 October 2014

Keywords: Multi-view range images Neighborhood Scanning Octree

ABSTRACT

The processing technologies of multi-view range images (MRIs) scanned by three-dimensional (3D) laser scanners, structured light scanners and laser radars (Ladars) are current research hotspot. Most of the processing such as denoising, integration and surface reconstruction are performed in local neighborhood. Thus, fast and precise query of the local neighborhoods of the 3D point data in MRIs is very important. Due to measurement accuracy and alignment error, there are gaps in overlapping regions and through theoretical analysis and experimental verification, we notice that the gaps which may result in loss of local neighborhood information have great influence on the neighborhood query whereas the previous methods ignore it. Thereby, a novel local neighborhood which is named cylindrical neighborhood (CYND) is proposed. Its searching procedures are described in detail. Compared with the previous methods, our CYND expands the searching scope along the directions of normal vectors of the 3D point data, hence eliminating the impact of gaps. The widely used and well-implemented ANN library was employed for a comparison study and the experimental results demonstrate the validity and superiority of our CYND. With extensive application of 3D optical scanning technologies, this novel neighborhood will have a wide application prospect.

© 2014 Elsevier Ltd. All rights reserved.

1. Introduction

3D scanning technologies and devices are widely used in industry [1]. The scanning devices such as 3D-laser scanners, structured light scanners and laser radars (Ladars) are extremely fast in data acquisition [2-4]. Whereas, these scanning devices usually have limited field of view and huge amounts of multi-view range images (MRIs) have to be captured from different views to reconstruct the object surfaces. The processing of MRIs such as denoising [5], integration [6] and surface reconstruction [7] are current research hotspot and these operations are often performed in local neighborhood. Thus, it is necessary to search neighborhoods of the 3D point data in MRIs. In general, the k-nearest neighbors, binary space partition (BSP) neighbors and voronoi neighbors are three types of neighborhoods which are usually employed [8]. Among them, the k-nearest neighbors is the most popular neighborhood widely used in processing of MRIs. The latter two neighborhoods are subsets of the *k*-nearest neighbors.

For a 3D point data \mathbf{P} , its k-nearest neighbors are defined as an ordered set of 3D point data $\Omega = \{\mathbf{P}_i | || \mathbf{P}_i - \mathbf{P}|| \le || \mathbf{P}_{i+1} - \mathbf{P}|| \}$, $0 \le i < N-1$, where N is the number of 3D point data in the set Ω and \mathbf{P}_i is a neighbor of \mathbf{P} . Indeed, the set Ω defines a sphere S

centered at **P** with radius $r = \|\mathbf{P}_{N-1} - \mathbf{P}\|$ such that the 3D point data P_i is a neighbor of P if and only if it is inside S (i.e., meeting the Euclidean distance criterion $\|\mathbf{P}_i - \mathbf{P}\| \le r$). So the *k*-nearest neighbors can also be regarded as a spherical neighborhood (SPND). The SPND of a 3D point data can be searched by means of a binary searching tree or an octree. There are some open source libraries such as ANN library [9] and FLANN [10] can be found on the internet. For a 3D point data in a single range image or nonoverlapping regions of MRIs, in most of the cases, its SPND contains appropriate information for any local processing. However, in overlapping regions of MRIs, due to measurement accuracy and alignment error, there are gaps among different MRIs [11]. The gap of a discrete 3D point in the overlapping areas is defined as the distance of the point to other surfaces along its normal vector. Fig. 1 shows the gap of **P** produced as a result of alignment error. In general, if there is only translation along the scanning direction (the Z-axis in Fig. 1), almost evenly distributed gaps are generated (Fig. 1(a)). In other situations (Fig. 1(b)-(d)), variable gaps are produced. The gaps in the overlapping areas of MRIs would result in loss of some neighbors.

As shown in Fig. 2(a), the two MRIs $scan_1$ and $scan_2$ have a constant gap of G that cause the neighboring 3D point data \mathbf{P}_i fall outside of the searching sphere and the larger the gap G is, the more the neighbors lose. An alternative scheme is increasing the searching radius r until all missed neighboring points are covered. In other words, increase the neighborhood. Whereas, large

^{*} Corresponding author.

E-mail address: xjtushbq@163.com (B.-Q. Shi).

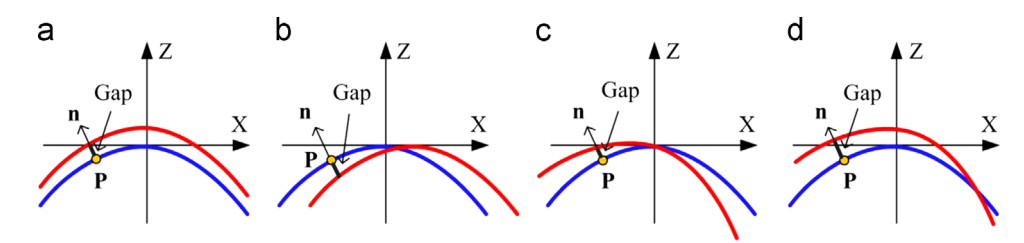


Fig. 1. The gaps produced by incorrect transformation during alignment (illustrated in 2D): (a) translation along *Z* direction, (b) translation along *X* direction, (c) rotation, and (d) combination of translation and rotation. The blue line represents the fixed scan and the red line represents the transformed scan. The gap of **p** is represented by the black thick line between the two scans along its normal vector direction. (For interpretation of the references to color in this figure legend, the reader is referred to the web version of this article.)

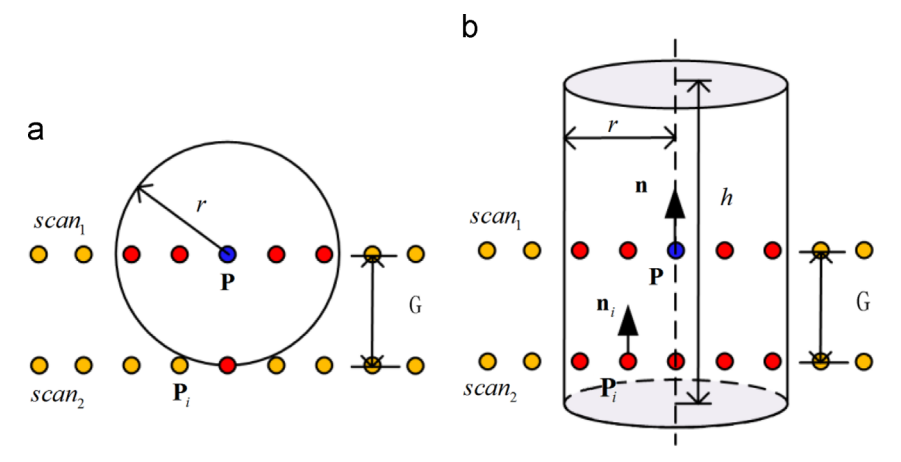


Fig. 2. Influence of gaps to the neighborhood of 3D point data in overlapping regions of MRIs. For better understand, a constant gap *G* is applied to the two MRIs *scan*₁ and *scan*₂. The yellow dots represent the 3D point data in MRIs, the blue dot represents the 3D point data **P**, and the red dots represent the (a) spherical neighbors and (b) cylindrical neighbors of **P**. (For interpretation of the references to color in this figure legend, the reader is referred to the web version of this article.)

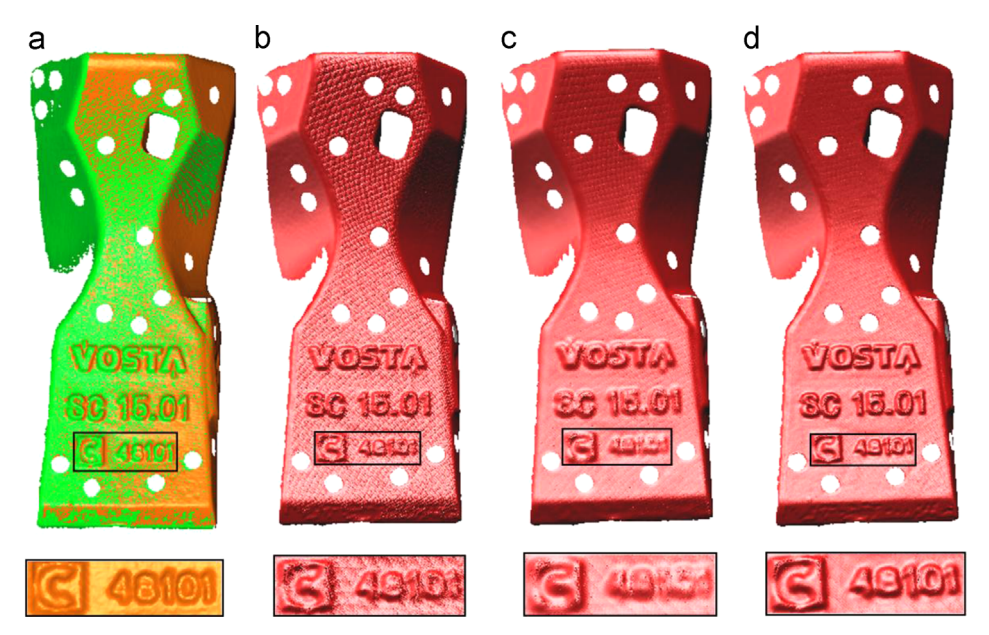


Fig. 3. MLS surface reconstruction [7] results of two partially overlapping MRIs of a bucket model. (a) The original two MRIs, (b) and (c) the MLS reconstruction surfaces by using the ANN library [9] for neighborhood query with parameter r=2.0 mm and r=4.0 mm respectively, (d) the MLS reconstruction surface by using our CYND for neighborhood query with parameters r=2.0 and h=2r. The enlargement figure in (a) only shows the small letters on the surface of the orange MRI, the small letters on the surface of the green MRI are omitted for better observation. (For interpretation of the references to color in this figure legend, the reader is referred to the web version of this article.)

neighborhood would blur small features for most of the local processing operators [7,9]. Fig. 3(b) and (c) gives an example of MLS surface reconstruction [7] of two MRIs of a bucket model (Fig. 3(a)) with different searching radius. By observing the enlargement figure

of the small letters in the overlapping areas, we can see that small features are blurred when the searching radius increased though the flat regions become smoother. Fig. 4(b) and (c) shows bilateral denoising [5] of two partially overlapping MRIs of a Yi tiger

Download English Version:

https://daneshyari.com/en/article/734823

Download Persian Version:

https://daneshyari.com/article/734823

<u>Daneshyari.com</u>